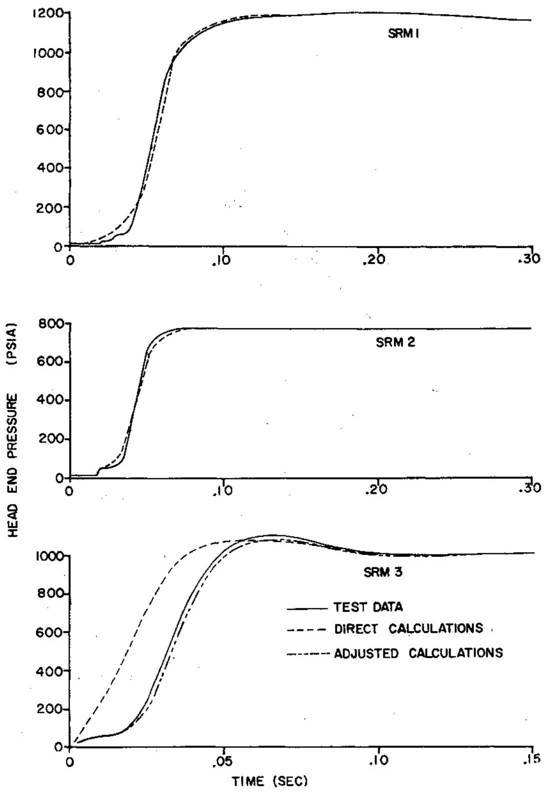

Fig. 4 Comparison of calculated chamber pressure with test results.

experimental results: $v_f = 3650$ in./sec yielded best agreement and was chosen for use in the first numerical example, and then applied to the other two numerical examples. The resulting comparisons are shown in Fig. 4. Two calculations are indicated for SRM3. In the first calculation the initial pressure rise occurred too soon. To investigate this, a pressure-time trace was calculated in which only the igniter furnished pressurization to the SRM. This trace was identical to the test trace for the first 16 msec. An adjusted trace was then computed in which the grain was first ignited after 16 msec. The "adjusted" curve in Fig. 4 agrees well with the test trace.

The transient ignition problem as studied herein can be divided into two phases: flame-spreading and chamber-filling. The flame-spreading portion of the $P_c(t)$ trace begins with zero slope and arcs upward to a position where the slope is approximately a maximum. The chamber-filling interval is the interval between complete ignition of the propellant surface and the time at which essentially steady chamber conditions are reached; it occupies the larger part of the ignition transient time. It is notable that $(dP_c/dt)_{\max}$ and $P_{c\max}$, which are the most important factors to be determined, are predicted quite well for all three motors, apparently because the chamber-filling phase is more important than the flame-spreading phase. Also, even for SRM 3, the analysis yields at least a first estimate of the transients during the initial phase.

Refinements to this analysis are possible. The variation of gaseous properties throughout the grain length could be more accurately determined by dividing the grain into short segments and solving the momentum, energy, and state equations in turn for each segment by an iterative technique until an over-all mass balance is achieved. An erosive burning law could also be included.

References

[1] Price, E. W. et al., "Theory of Ignition of Solid Propellants," *AIAA Journal*, Vol. 4, No. 7, July 1966, pp. 1153–1181.

[2] de Sota, S. and Friedman, H. A., "Flame Spreading and Ignition Transients in Solid Grain Propellants," *AIAA Journal*, Vol. 3, No. 3, March 1965, pp. 405–412.

[3] Barrère, M. et al., *Rocket Propulsion*, 1st ed., Elsevier, Amsterdam, 1960, pp. 237–243 and pp. 255–256.

[4] Ralston, A., *A First Course in Numerical Analysis*, 1st ed., McGraw-Hill, New York, 1965, p. 200.

Angle of Attack and Lateral Rate for Nearly Circular Re-Entry Motion

Mark M. Lotkin*
General Electric Company, Philadelphia, Pa.

Nomenclature

A = reference area of vehicle
a = scale height
C_D = drag coefficient
$C_{M\alpha}$ = pitching moment coefficient slope
d = reference diameter of vehicle
H = $h_0 - h$
h = geometric altitude; $h_0 = h(t_0)$ at re-entry
I_x, I_y = roll and pitch moments of inertia
k = $AC_D/am \sin\gamma_0$ = "drag" parameter
m = mass of vehicle
q_∞ = $\rho V^2/2$ = dynamic pressure
s = total lateral angular rate
t = time
V = relative velocity of vehicle
γ = flight path angle
δ = total angle of attack
ρ = density of air
ω = body-fixed frequency of vehicle

Subscripts

$(\ )_0$ = at arbitrary altitude h_0; see Eqs. (7)
$(\ )_s$ = at sea level, $h_s = 0$

Introduction

In a previous article[1] there was derived a set of ordinary first-order differential equations for the total angle-of-attack δ and the relative roll angle μ in terms of the vehicle's roll, pitch, and yaw rates. These equations apply to the exosphere as well as the atmosphere, and for angles of arbitrary magnitude. In this Note these basic equations are applied to the case of nearly circular angle-of-attack motion during re-entry, for small angles of attack. The use of well-known expressions for the frequencies of the lateral rates permits an integration of the differential equation for a mean value of δ, leading to an expression of a mean total lateral rate as well. The general expressions thus obtained are applied to cases that are typical of the high-altitude trajectory of advanced re-entry vehicles, leading to approximations of potential utility in simulations of pertinent trajectories. Finally, a typical example is given.

Differential Equations

In Ref. 1 it was shown that δ and μ satisfy

$$\dot{\delta} = s \sin(\mu - \epsilon) \tag{1}$$

$$\dot{\mu} = -p + (s/\tan\delta) \cos(\mu - \epsilon) \tag{2}$$

with

$$s^2 = q^2 + r^2 \qquad \tan\epsilon = r/q \tag{3}$$

Received December 23, 1969.

* Consultant, Re-entry and Environmental Systems Division.

Equations (1) and (2) are readily transformed into an equivalent set of equations by the introduction of the angles

$$\eta = (\pi/2) - \epsilon \qquad v = (\pi/2) - \mu \tag{4}$$

where v denotes the frequently used "windward meridian angle." There results

$$\dot{\delta} = -s \sin(v - \eta) \tag{5}$$

$$\dot{v} = p - (s/\tan\delta) \cos(v - \eta) \tag{6}$$

We shall fix the solution of Eqs. (5) and (6) by specifying that at the time $t = t_0$,

$$\bar{\delta}(t_0) = \delta_0, v(t_0) = 0 \tag{7}$$

with $\bar{\delta}$ denoting a mean value. Equations (5) and (6) are valid for arbitrary values of δ.

In general, pitch and yaw rates q and r may be represented in the form

$$q = s \sin\omega(t - t_0) \tag{8}$$

$$r = s \cos\omega(t - t_0) \tag{9}$$

and

$$\tan\eta = \tan\omega(t - t_0)$$

so that

$$\eta = \omega(t - t_0) + n\pi, n = 0, \pm 1, \pm 2, \ldots \tag{10}$$

For small δ, the body-fixed frequencies are given by

$$\omega = p(1 - I_x/2I_y) \pm W \tag{11}$$

with

$$W^2 = (pI_x/2I_y)^2 - (Ad/I_y)q_\infty C_{M\alpha} \tag{12}$$

Nearly Circular Motion

Circular motion is encountered when δ = constant for all times. In such a case, from Eqs. (5) and (10),

$$v = \eta = \omega(t - t_0) \tag{13}$$

In the exosphere, where $\rho \approx 0$ (hence, $q_\infty \approx 0$), by Eq. (11),

$$\omega = p \text{ or } p(1 - I_x/I_y)$$

From Eq. (7), for circular motion, at $h = h_0$,

$$s_0/\tan\delta_0 = p - \omega$$

or, by Eq. (11),

$$s_0/\tan\delta_0 = pI_x/I_y \tag{14}$$

We define "nearly circular" motion as one where

$$v = \omega(t - t_0) + \epsilon(t - t_0) \tag{15}$$

where ϵ is a constant, and $\epsilon \ll |p|$ by definition. In such a case we are permitted to put

$$\sin(v - \eta) = \epsilon(t - t_0) \tag{16}$$

$$\cos(v - \eta) = 1 \tag{17}$$

Denoting the resulting solution of Eqs. (5) and (6) by $\bar{\delta}$, $\bar{s}$, we have, from Eq. (6)

$$\bar{s}/\bar{\delta} = F(t) = p - \omega - \dot{\omega}(t - t_0) \tag{18}$$

Introducing the resulting expression for $\bar{s}$ into Eq. (5),

$$\dot{\bar{\delta}}/\bar{\delta} = -\epsilon F(t - t_0) \tag{19}$$

It follows that

$$\frac{\bar{\delta}(t)}{\bar{\delta}_0} = \exp\left[-\epsilon \int_{t_0}^{t} F(t - t_0)dt\right] \tag{20}$$

For $h < h_0$, where $h_0 = h(t_0)$, it is convenient here to employ the geometric altitude $H = h_0 - h$, as the independent variable. Since $H = \dot{H}(t - t_0)$, $\dot{H} = V \sin\gamma$, Eq. (20) may be expressed as

$$\bar{\delta}(H)/\bar{\delta}_0 = \exp[-\epsilon J(H)] \tag{21}$$

where

$$J(H) = \int_0^H \left[\frac{H}{(\dot{H})^2}\right] F(H)dH \tag{22}$$

$$F(H) = p - \omega - H(d\omega/dH) \tag{23}$$

The quantity ϵ can be estimated readily if it is known that $\bar{\delta} = \bar{\delta}_f$ for $H = H_f$. In such a case, clearly,

$$\epsilon = \log(\bar{\delta}_0/\bar{\delta}_f)/J(H_f) \tag{24}$$

Finally, from Eqs. (18), $\bar{s}(H) = \bar{\delta}(H)F(H)$, for $F(H) \geq 0$. Hence,

$$\bar{s}/\bar{s}_0 = (\bar{\delta}/\bar{\delta}_0)[F(H)/F(H_0)] \tag{25}$$

In summary, for nearly circular motion, Eqs. (21–25) are used as follows. The time (or altitude) histories of h, V, γ, and ρ are obtained. The required additional inputs are A, d, I_x, I_y, as well as $\bar{\delta}_0$, $\bar{s}_0$, and $\bar{\delta}_f(h_f)$. The functions $C_{M\alpha}(h)$ and p may be provided either in tabular or analytical form. Then the following quantities are calculated, in order: 1) $\dot{p}$ and $(q_\infty C_{M\alpha})$, by numerical differentiation, 2) W by Eq. (12), and then $\dot{W}$, 3) $\dot{\omega} = [1 - (I_x/2I_y)]\dot{p} + \dot{W}$, and 4) Equations (23–24), (21), and (25), in that order.

We can obtain approximate expressions for the functions F and J when certain assumptions are made that apply to many stable, high-performance (high-ballistic parameter) re-entry vehicles for which $\bar{\delta}$ rapidly damps to small values:

1) The roll rate p is constant, such that for the first term of W,

$$p(I_x/2I_y)^2 \ll -(Ad/I_y)(q_\infty C_{M\alpha}) \tag{26}$$

2) C_D is constant.

3) $C_{M\alpha}$ is a slowly changing, negative function of altitude

$$C_{M\alpha}(H) = C_{M\alpha 0}e^{cH} \tag{27}$$

with $C_{M\alpha 0} < 0$, c small. For aerodynamically stable re-entry vehicles, c is negative.

4) The re-entry trajectory is straight. Then,

$$\dot{H} = V \sin\gamma_0 \tag{28}$$

Table 1 Illustrative example

H, kft	ρ, slug/ft³	V, fps	$C_{M\alpha}$*, rad⁻¹	$Q(H)$, sec⁻¹	$F(H)$, sec⁻¹	$J(H)$, sec	f	g, ft⁻¹	$\bar{\delta}$, deg	$\bar{s}$, deg/sec
0	4.96×10^{-9}	20,000	1.20	0.616	0.616	0	1.00	6.68×10^{-5}	8.00	2.00
100	3.81×10^{-7}	19,980	0.442	3.28	8.76	940	2.67	1.05×10^{-4}	6.80	24.08
200	2.94×10^{-5}	18,760	0.162	16.4	62.2	16,980	3.79	-3.16×10^{-4}	0.40	10.10
220	7.02×10^{-5}	17,180	0.133	21.0	67.5	24,310	3.22	...	0.11	3.08
240	1.67×10^{-4}	13,940	0.109	23.8	29.3	31,710	1.23	...	0.03	0.38
247	2.26×10^{-4}	12,260	0.102	23.5	−2.58	32,790	−0.11	...	(0.02)	...

5)
$$\rho(H) = \rho_0 e^{aH} \tag{29}$$

with a denoting a positive constant. It is shown in Ref. 2 that because of assumptions 2, 4, and 5,

$$V = V_0 e^{(\rho_0 - \rho)k/2} \tag{30}$$

with

$$k = AC_D/(am \sin\gamma_0) \tag{31}$$

With these assumptions we may express $F(H)$ in the form

$$F(H) = Q + H(dQ/dH) \tag{32}$$

where

$$Q = [(Ad/I_y)q_\infty C_{M\alpha}^*]^{1/2},\ C_{M\alpha}^* = -C_{M\alpha} \tag{33}$$

Thus,

$$F(H) = Q(H)f(H)$$

where

$$f(H) = 1 + (H/2)\varphi(H) \tag{34}$$

and

$$\varphi(H) = a(1 - k\rho) + c$$

Behavior of $\bar{\delta}$(H) and $\bar{s}$(H)

It is of general interest to investigate the capability of the approximate expressions to properly depict the well-known over-all behavior of $\bar{\delta}$ and $\bar{s}$ for a stable vehicle in the re-entry region $0 \leq H \leq H_s$. A stable vehicle is defined here as one for which δ rapidly decreases as the altitude decreases (H increases). For such a behavior of $\bar{\delta}$ it is clearly necessary that the total lateral rate $\bar{s}$ also assumes small values at low altitudes.

For the derivatives of $\bar{\delta}$ and $\bar{s}$ we obtain

$$d\bar{\delta}/dH = -\epsilon\bar{\delta}Qf(H)[H/(\dot{H})^2] \tag{35}$$

and

$$d\bar{s}/dH = (\tfrac{1}{2})\bar{\delta}Qg(H) \tag{36}$$

with

$$g(H) = (1 + f)\varphi(H) - H\psi(H) \tag{37}$$

and

$$\psi(H) = a^2k\rho + 2\epsilon Q(f/\dot{H})^2 \tag{38}$$

Note that $\psi(H) \geq 0$ always.

The behaviors of $\bar{\delta}$ and $\bar{s}$ are thus controlled by $f(H)$ and $g(H)$, respectively. For $H = 0$, $f(0) = 1$, and $g(0) = 2\varphi(0) = 2(a + c - ak\rho_0)$. On physical grounds it is known that $g(0) > 0$. Thus, in general, at $H = 0$, $d\bar{\delta}/dH = 0$, and $d\bar{s}/dh > 0$.

Since it is known on physical grounds that $\bar{s}$ must eventually become small, $\bar{s}(H)$ must always assume a maximum at some altitude $H = H_{ma}$. In order for $\bar{\delta}(H)$ to show a monotonic decrease in an altitude band it is necessary that $f(H)$ be positive in that altitude band.

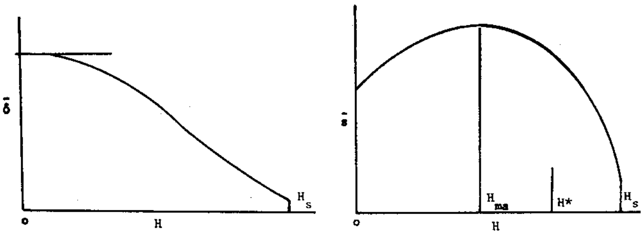

Fig. 1 Case Ib.

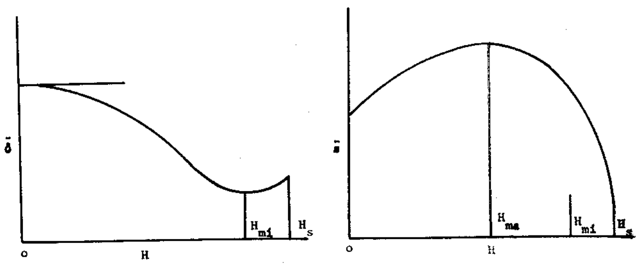

Fig. 2 Case II.

In discussing the behavior of $f(H)$ and $g(H)$, the comparison between the "drag" parameter k defined in Eq. (31), and the parameter

$$k_c = (1/a\rho_s)[a + c + (2/H_s)] \tag{39}$$

is of significance. Two different cases (and two subcases of case I) arise: Case I, $0 \leq k \leq k_c$. In this case $f(H) \geq 1 - (H/H_s) \geq 0$. Thus, $d\bar{\delta}/dH < 0$ for all H; $\bar{\delta}$ is a decreasing function of H everywhere. We can subdivide case I by introducing

$$k_s = (1/a\rho_s)(a + c),\ (k_s < k_c) \tag{40}$$

Case Ia, $0 \leq k \leq k_s$. Now $\varphi(H) \geq 0$ for all H, so that $f(H) \geq 1$. Also, $g(H_s) \geq -H_s\psi(H_s)$. As was stated previously, there must exist $H_{ma} < H_s$ at which $\bar{s}(H)$ assumes a maximum, i.e., $g(H_{ma}) = 0$. Case Ib, $k_s < k \leq k_c$. Now $\varphi(H_s) < 0$. There exists H^* so that $\varphi(H^*) = 0$. Consequently, $g(H^*) = -H^*\psi(H^*) < 0$. Thus, there must exist $H_{ma} < H^*$ for which $g(H_{ma}) = 0$, i.e., at which $\bar{s}(H)$ assumes a maximum. H^* may be calculated from the equation: $\rho(H^*) = (1/ak)(a + c)$. Case II, $k_c < k$. Now $\varphi(H_s) < -(2/H_s) < 0$, so that $f(H_s) < 0$. Since $f(0) = 1$, there exists H_{mi} such that $f(H_{mi}) = 0$; $\bar{\delta}(H)$ assumes a minimum at H_{mi}. It is noted that H_{mi} satisfies $H_{mi} = -2/\varphi(H_{mi})$. This minimum is artificial, caused by the mathematical approximation. In practice H_{mi} will occur at a sufficiently low altitude so as not to affect the over-all qualitative descriptions of $\bar{\delta}$ and $\bar{s}$. At H_{mi}, $g(H_{mi}) = -[(2/H_{mi}) + H_{mi}\psi(H_{mi})] < 0$. There exists $H_{ma} < H_{mi}$ for which $g(H_{ma}) = 0$; $\bar{s}(H)$ assumes a maximum at H_{ma}.

The cases Ib and II are depicted in Figs. 1 and 2. High-performance re-entry vehicles are characterized by relatively small values of k. The behavior of $\bar{\delta},\bar{s}$ is then typified by case Ia.

Illustrative Example

The approximate solutions resulting from the assumptions (26–29) will be determined for a vehicle performing nearly circular δ motion during re-entry, having the following properties: $m = 100\pi$ lb m, $d = 2$ ft, $A = \pi$ ft², $I_x = 2$ slug-ft², $I_y = 20$ slug-ft², $C_D = 0.2$, and $C_{M\alpha} = -1.2e^{-H/10^6}$ rad⁻¹.

The high-altitude conditions assumed are: $h_0 = 300{,}000$ ft, $V_0 = 20{,}000$ fps, $\gamma_0 = 20°$ below local horizontal, $\bar{\delta}_0 = 8°$, $\bar{s}_0 = 2$ deg/sec, $p = 2\pi$ rad/sec, and $\rho_0 = 4.96 \times 10^{-9}$ slug/ft³ (1966 U.S. Standard Atmosphere, 15° latitude).

For the in-flight condition, we assume that at $h_f = 100$ kft, $\bar{\delta}_f = 0.4°$. With $\rho_s = 2.26 \times 10^{-3}$ slug/ft³, it is seen that $a = 4.34 \times 10^{-5}$ ft⁻¹. Next, by Eq. (31), $k = 4335$ ft³/slug, and, by Eq. (39), $k_c = 408$ ft³/slug. Thus, we have case II. The altitude H_{mi} at which $\bar{\delta}$ assumes a minimum is given by $H_{mi} = -2/\varphi(H_{mi})$; it turns out that $H_{mi} \approx 247$ kft, or $h_{mi} \approx 53$ kft. Further, $Q(H) = 0.40V(\rho C_{m\alpha}^*)^{1/2}$ sec⁻¹. A condensed listing of the calculations is given in Table 1.

The parameter ϵ, determined by Eq. (24) and the in-flight condition, is found to be $\epsilon = 1.76 \times 10^{-4}$ rad/sec. The constraint Eq. (15), $\epsilon \ll |p|$, is thus certainly satisfied for the example. The altitude H_{ma} at which $\bar{s}$ assumes a maximum can be calculated from the equation $g(H_{ma}) = 0$; it turns out that $H_{ma} \approx 125$ kft, i.e., $h_{ma} \approx 175$ kft.

Conclusion

General expressions are provided that permit the determination during re-entry of the total angle-of-attack $\bar{\delta}$ and the total lateral rate $\bar{s}$ of a vehicle performing nearly circular motion, if the histories of such trajectory parameters as relative velocity, flight path angle, and the pitching moment coefficient slope of the vehicle are known. With certain simplifying assumptions that are reasonable for many high ballistic-coefficient vehicles, approximate solutions are obtained that simulate the nominal behavior of $\bar{\delta}$ and $\bar{s}$ in a satisfactory manner.

References

[1] Lotkin, M., "Determination of Angle of Attack from Rotational Body Rates," *Journal of Spacecraft and Rockets*, Vol. 4, No. 10, Oct. 1967, pp. 1333–1338.

[2] Allen, H. J., "Motion of a Ballistic Missile Angularly Misaligned with the Flight Path Upon Entering the Atmosphere and its Effect Upon Aerodynamic Heating, Aerodynamic Loads, and Miss Distance," TN 4048, Oct. 1957, NACA.

Probability of Rescue in Emergency Return Missions

S. T. Chu* and A. R. Nagy Jr.†
Aerospace Corporation, El Segundo, Calif.

Nomenclature

f_c = specific fuel consumption for aircraft cruising (for round trip from and back to the recovery aircraft station, twice the value of the conventional-cruising specific fuel consumption in lb/hr)
f_L = specific fuel consumption for aircraft loitering
K = kernel function defined in Eq. (10)
p = return probability
p_{SR} = probability of successful rescue operation (assuming unit reliability of pickup)
r = search radius, measured along a great circle arc
r_a = $V_a(t_E + t_1)$
r_{a1} = $V_a(t_E + t_{w1} - t_D)$
r_{a2} = $[V_a f_L/(f_c - f_L)][(w_f/f_L) + t_d - t_E - t_1]$
r' = intersection of $t_{s1}\{r\}$ and $t_{s2}\{r\}$ in which the portion of t_{s1} lying below zero is replaced by $t_{s1} = 0$
R = maximum range of rescue aircraft = $V_a t_{cmx}$
t_1 = allowable in-orbit waiting time
t_c = aircraft cruising time; $t_{cmx} = (w/f_{cf})$
t_d = takeoff delay time of rescue aircraft, time between decision-to-return and aircraft takeoff
t_E = spacecraft reentry time
t_L = aircraft loiter time; $t_{Lmx} = (w_f/f_L)$
t_θ = orbital period
t_s = spacecraft waiting time
t_{s1},t_{s2} = defined in Eqs. (8) and (9), respectively
t_w = water immersion time; t_{w1} = allowable water immersion time of spacecraft
V_a = cruising speed of rescue aircraft
w_f = total fuel available for rescue aircraft for cruising and loitering
θ = orbital inclination

Received January 8, 1970; revision received March 2, 1970. This work was performed for the Space and Missile Systems Organization, Air Force Systems Command, under Contract F04701-69-C-0066.

* Director, Resource and Systems Analysis Office, Systems Planning Division. Associate Fellow AIAA.

† Member of Technical Staff, Resource and Systems Analysis Office, Systems Planning Division. Member AIAA.

Introduction

A successful rescue of spacecraft or an escape capsule requires that the spacecraft returns from orbit to one of the recovery areas and that the rescue aircraft locates the spacecraft and picks up the distressed astronauts at the splash point; i.e., matching a time sequence for the spacecraft with a corresponding time sequence for the rescue aircraft. This Note summarizes a method of analysis[1] that will aid in 1) determining design criteria for spacecraft, 2) tradeoff studies in recovery planning, 3) establishment of requirements for recovery forces, and 4) selection of recovery sites. Sample results are included.

Probability of Rescue Success

Let us consider a ring on the Earth's surface formed by the difference between two concentric recovery circles of radius r and $r + dr$. The return probability of a spacecraft to this ring or a collection of such rings for multiple recovery stations within an allowable in-orbit waiting time, t_1, is given by

$$dp(r,t_1) = p(r + dr,t_1) - p(r,t_1) \tag{1}$$

where r is the limiting recovery radius measured along an Earth great circle arc. This definition implicitly assumes successful deorbit and re-entry. For a specific return operation, the recovery radius will take a value between 0 and r and the actual in-orbit waiting time t_s will lie between 0 and t_1 depending upon the position of the spacecraft at the time of return decision.

The individual elements of a rescue operation and their interactions may best be appreciated by examining a time sequence of the operation; for the spacecraft this sequence includes t_s, the time of re-entry from deorbit to splashdown t_E, and the water immersion time t_w, whereas for the rescue aircraft it includes the delay time t_d, the cruise time t_c, and the loiter time t_L. The re-entry time, t_E, may be considered as a fixed quantity determined by the orbit altitude, spacecraft characteristics, and re-entry conditions, and t_w varies between zero and its allowable t_{w1}; thus,

$$t_E = \text{fixed},\ 0 \leq t_s \leq t_1,\ 0 \leq t_w \leq t_{w1} \tag{2}$$

For the rescue aircraft, the t_d may be attributable to the time for sending messages of return decision to the recovery force and the alert time for aircraft takeoff; t_c and t_L are varying quantities and are related to each other through a fixed amount of fuel carried by the aircraft

$$w_f = f_c t_c + f_L t_L = \text{fixed} \tag{3}$$

Since the specific fuel consumption for loitering, f_L, is expected to be smaller than that for cruise, f_c, the limits within which t_c and t_L can vary are, therefore, different and are given by

$$0 \leq t_c \leq t_{cmx} \qquad 0 \leq t_L \leq t_{Lmx} \tag{4}$$

where $t_{cmx} = w_f/f_c$ and $t_{Lmx} = w_f/f_L$. For a successful rescue operation, two conditions must be met: the aircraft must arrive at the splash point no later than a fixed t_{w1} hr after the spacecraft splashes into the water and, if the rescue aircraft arrives at the splash point first, it must loiter about this location until the spacecraft splashes down; i.e.,

$$t_c + t_d \leq t_s + t_E + t_{w1} \tag{5}$$

$$t_c + t_d + t_L \geq t_s + t_E \tag{6}$$

By using Eq. (3), the inequality of Eq. (6) may be written as

$$t_c + t_d + w_f/f_L - t_c f_c/f_L \geq t_s + t_E \tag{7}$$

Two varying quantities, t_c and t_s, play different roles in the analysis; t_c may be considered as an independent variable, and for a specific value of t_c, the probability of successful